# DIGITAL REACTION-DIFFUSION SYSTEM AND ITS APPLICATION TO BIO-INSPIRED TEXTURE IMAGE PROCESSING

*Koichi Ito*[†], *Takafumi Aoki*[†] *and Tatsuo Higuchi*[††]

[†] Graduate School of Information Sciences,
Tohoku University,
Aoba 05, Sendai, 980-8579 Japan
Phone: +81-22-217-7169, FAX: +81-22 263-9308,
E-mail: ito@aoki.ecei.tohoku.ac.jp

[††] Department of Electronics,
Tohoku Institute of Technology,
Sendai 982-8577 Japan

## ABSTRACT

This paper presents a digital reaction-diffusion system (DRDS) – a model of a discrete-time discrete-space reaction-diffusion dynamical system – for designing new image processing algorithms inspired by biological pattern formation phenomena. The original idea is based on the Turing's model of pattern formation, which is widely known in mathematical biology. The DRDS is useful for generating biological textures, patterns and structures. This paper describes the design of DRDS for image processing tasks, such as biological texture generation, fingerprint image restoration and shortest path search.

## 1. INTRODUCTION

Living organisms can create a remarkable variety of patterns and forms from genetic information. In embryology, the development of patterns and forms is sometimes called *Morphogenesis*. In 1952, Alan Turing suggested that a system of chemical substances, called *morphogens*, reacting together and diffusing through a tissue, is adequate to account for the main phenomena of morphogenesis [1]. From an engineering viewpoint, the insights into morphogenesis provide important concepts for devising a new class of intelligent signal processing algorithms inspired by biological pattern formation phenomena [2]–[4].

In general, most of computational models of biological pattern formation are described by continuous-time continuous-space reaction-diffusion equations, and hence can not be directly handled by the theory of digital signal processing. Addressing this problem, we propose a *Digital Reaction-Diffusion System* (DRDS) — a model of a discrete-time discrete-space reaction-diffusion dynamical system, which is useful for designing new types of signal processing algorithms based on biological pattern formation mechanism [5], [6]. Using the DRDS, mathematical models of morphogenesis can be understood by multidimensional digital signal processing theory. In this paper, we present the basic framework of DRDS, and its application to computer graphics, fingerprint image restoration and shortest path search.

## 2. DIGITAL REACTION-DIFFUSION SYSTEM (DRDS)

A Digital Reaction-Diffusion System (DRDS) – a model of a discrete-time discrete-space reaction-diffusion dynamical system – can be naturally derived from the original reaction-diffusion system defined in continuous space and time. The general $M$-morphogen reaction-diffusion system with two-dimensional (2-D) space indices $(r_1, r_2)$ is written as

$$\frac{\partial \tilde{\boldsymbol{x}}(t, r_1, r_2)}{\partial t} = \tilde{\boldsymbol{R}}(\tilde{\boldsymbol{x}}(t, r_1, r_2)) + \tilde{\boldsymbol{D}}\nabla^2 \tilde{\boldsymbol{x}}(t, r_1, r_2), \tag{1}$$

where

$\tilde{\boldsymbol{x}} = [\tilde{x}_1, \tilde{x}_2, \cdots, \tilde{x}_M]^T$,
  $\tilde{x}_i$: concentration of the $i$-th morphogen,
$\tilde{\boldsymbol{R}}(\tilde{\boldsymbol{x}}) = [\tilde{R}_1(\tilde{\boldsymbol{x}}), \tilde{R}_2(\tilde{\boldsymbol{x}}), \cdots, \tilde{R}_M(\tilde{\boldsymbol{x}})]^T$,
  $\tilde{R}_i(\tilde{\boldsymbol{x}})$: reaction kinetics for the $i$-th morphogen,
$\tilde{\boldsymbol{D}} = diag[\tilde{D}_1, \tilde{D}_2, \cdots, \tilde{D}_M]$,
  $diag$: diagonal matrix,
  $\tilde{D}_i$: diffusion coefficient of the $i$-th morphogen.

We now sample a continuous variable $\tilde{\boldsymbol{x}}$ in (1) at the time sampling interval $T_0$, and at the space sampling intervals $T_1$ and $T_2$. Assuming discrete time-index to be given by $n_0$ and discrete space

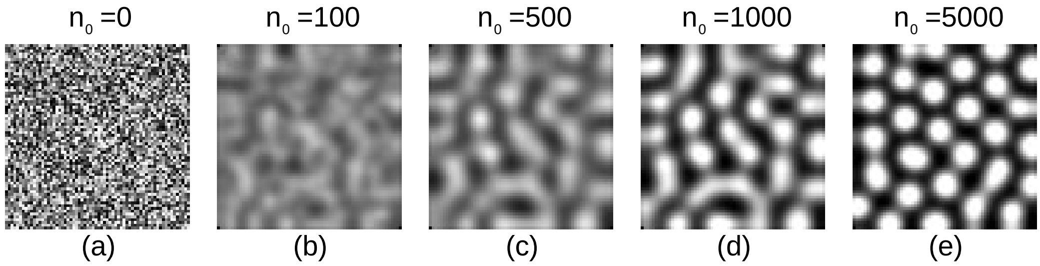


Figure 1: Formation of a spot pattern using DRDS with Brusselator reaction kinetics.

indices to be given by $(n_1, n_2)$, we have

$$\boldsymbol{x}(n_0, n_1, n_2) = \tilde{\boldsymbol{x}}(n_0T_0, n_1T_1, n_2T_2). \qquad (2)$$

Using this discritization, the general DRDS can be obtained as

$$\begin{aligned}\boldsymbol{x}(n_0{+}1, n_1, n_2) &= \boldsymbol{x}(n_0, n_1, n_2)\\ &+\boldsymbol{R}(\boldsymbol{x}(n_0, n_1, n_2)) + \boldsymbol{D}(l * \boldsymbol{x})(n_0, n_1, n_2), \qquad (3)\end{aligned}$$

where

$$\begin{aligned}\boldsymbol{x} &= [x_1, x_2, \cdots, x_M]^T,\\ \boldsymbol{R} &= T_0\tilde{\boldsymbol{R}} = [R_1(\boldsymbol{x}), R_2(\boldsymbol{x}), \cdots, R_M(\boldsymbol{x})]^T,\\ \boldsymbol{D} &= T_0\tilde{\boldsymbol{D}} = diag[D_1, D_2, \cdots, D_M],\\ & l(n_1, n_2)\\ &= \begin{cases} \frac{1}{T_1^2} & (n_1, n_2) = (-1, 0), (1, 0)\\ \frac{1}{T_2^2} & (n_1, n_2) = (0, -1), (0, 1)\\ -2(\frac{1}{T_1^2} + \frac{1}{T_2^2}) & (n_1, n_2) = (0, 0)\\ 0 & \text{otherwise,}\end{cases}\end{aligned}$$

and $*$ is the spatial convolution operator defined as

$$\begin{aligned}&(l * \boldsymbol{x})(n_0, n_1, n_2)\\ &= \begin{bmatrix} (l * x_1)(n_0, n_1, n_2)\\ (l * x_2)(n_0, n_1, n_2)\\ \vdots\\ (l * x_M)(n_0, n_1, n_2)\end{bmatrix}\\ &= \begin{bmatrix} \sum_{p_1=-1}^{1}\sum_{p_2=-1}^{1} l(p_1, p_2)x_1(n_0, n_1 - p_1, n_2 - p_2)\\ \sum_{p_1=-1}^{1}\sum_{p_2=-1}^{1} l(p_1, p_2)x_2(n_0, n_1 - p_1, n_2 - p_2)\\ \vdots\\ \sum_{p_1=-1}^{1}\sum_{p_2=-1}^{1} l(p_1, p_2)x_M(n_0, n_1 - p_1, n_2 - p_2)\end{bmatrix}.\end{aligned}$$

The DRDS described by Eq. (3) can be understood as a 3-D nonlinear digital filter. We first store an initial (input) image in a specific morphogen, say $x_i(0, n_1, n_2)$, at time 0. After computing the dynamics for $n_0$ steps, we can obtain the output image from one of the $M$ morphogens, say $x_i(n_0, n_1, n_2)$, at time $n_0$. In general, linear digital filters with guaranteed stability are widely used in many signal processing applications. In our application, however, we employ the DRDS with nonlinear reaction kinetics $\boldsymbol{R}(\boldsymbol{x})$ satisfying the diffusion-driven instability condition [5]. In this case, DRDS becomes an unstable 3-D nonlinear digital filter having significant pattern formation capability.

In this paper, we use the two-morphogen DRDS ($M = 2$) with the Brusselator reaction kinetics, which is one of the most widely studied chemical oscillators [7]. The two-morphogen Brusselator-based DRDS is defined as follows:

$$\begin{aligned}\begin{bmatrix} x_1(n_0{+}1, n_1, n_2)\\ x_2(n_0{+}1, n_1, n_2)\end{bmatrix} &= \begin{bmatrix} x_1(n_0, n_1, n_2)\\ x_2(n_0, n_1, n_2)\end{bmatrix}\\ &+ \begin{bmatrix} R_1(x_1(n_0, n_1, n_2), x_2(n_0, n_1, n_2))\\ R_2(x_1(n_0, n_1, n_2), x_2(n_0, n_1, n_2))\end{bmatrix}\\ &+ \begin{bmatrix} D_1(l * x_1)(n_0, n_1, n_2)\\ D_2(l * x_2)(n_0, n_1, n_2)\end{bmatrix}, \qquad (4)\end{aligned}$$

where

$$\begin{aligned}R_1(x_1, x_2) &= T_0\left\{k_1 - (k_2 + 1)x_1 + x_1^2x_2\right\},\\ R_2(x_1, x_2) &= T_0\left(k_2x_1 - x_1^2x_2\right).\end{aligned}$$

In this paper, we consider the parameter set: $k_1 = 2$, $k_2 = 4$, $T_0 = 0.01$, $D_1 = T_0$ and $D_2 = 5T_0$. In this case, the DRDS shows the spot pattern formation from random initial concentration as shown in Fig. 1. By changing the parameters, we can generate various biological patterns.

## 3. FINGERPRINT RESTORATION

In this section, we show the fingerprint image enhancement/restoration using DRDS.

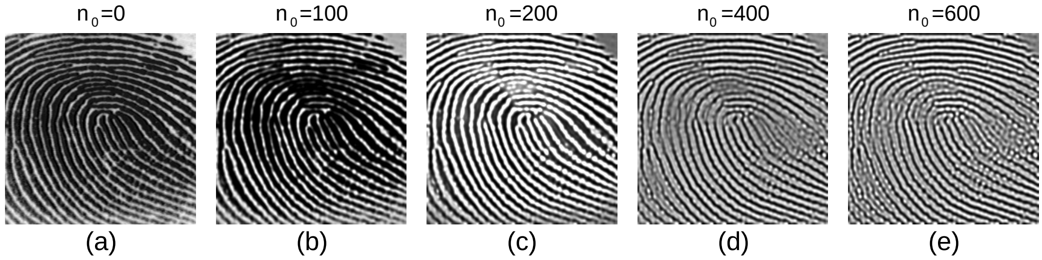


Figure 2: Enhancement of a fingerprint image.

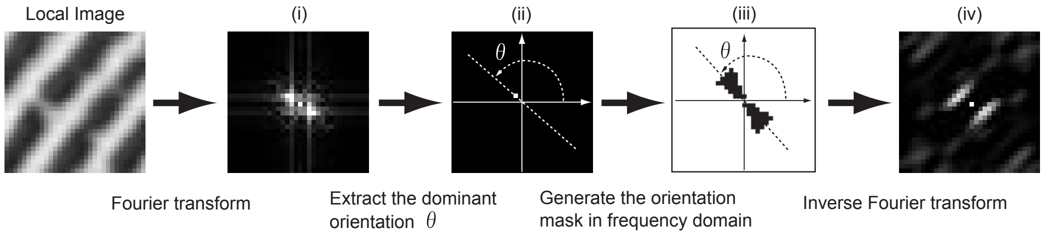


Figure 3: Generation of the orientation mask.

The two-morphogen DRDS (4) can be used to enhance fingerprint patterns [5]. We first set the initial fingerprint image in $x_1(0, n_1, n_2)$, at time 0. Note that spatial sampling parameters $T_1$ and $T_2$ should be adjusted according to the inherent spatial frequency of the given fingerprint image. The dynamics (4) has the equilibrium $(x_1, x_2) = (2, 2)$, and the variation ranges of variables $(x_1, x_2)$ are bounded around the equilibrium point as $1 \le x_1 \le 3$ and $1 \le x_2 \le 3$ in the case of given parameter set. Hence, we first scale the [0,255] gray-scale fingerprint image into [1,3] range. The scaled image becomes the initial input $x_1(0, n_1, n_2)$, while the initial condition of the second morphogen is given by $x_2(0, n_1, n_2) = 2$. The zero-flux Neumann boundary condition is employed for computing the dynamics. After $n_0$ steps of the DRDS computation, we obtain $x_1(n_0, n_1, n_2)$ as the output image, which is scaled back into the [0,255] gray-scale image to produce the final output.

Figure 2 shows the enhancement of a fingerprint image using the DRDS. Our initial observation, however, shows that the DRDS with a spatially isotropic diffusion term of (4) often produces some broken ridge lines in processing fingerprint images as shown in Fig. 2(e), since it does not take account of the local orientation of ridge flow. In order to solve this problem, the next section defines an *adaptive DRDS* model, in which we can use the local orientation of the ridge flow in a fingerprint image to guide the action of DRDS. This can be realized by introducing orientation masks to be convolved with the diffusion terms in DRDS (4).

We modify the definition of the simple two-morphogen DRDS (4) to have an adaptive DRDS dedicated to fingerprint restoration tasks. The two-morphogen adaptive DRDS with the Brusselator reaction kinetics can be written as

$$\begin{aligned}\begin{bmatrix} x_1(n_0+1, n_1, n_2) \\ x_2(n_0+1, n_1, n_2) \end{bmatrix} &= \begin{bmatrix} x_1(n_0, n_1, n_2) \\ x_2(n_0, n_1, n_2) \end{bmatrix} \\ &+ \begin{bmatrix} R_1(x_1(n_0, n_1, n_2), x_2(n_0, n_1, n_2)) \\ R_2(x_1(n_0, n_1, n_2), x_2(n_0, n_1, n_2)) \end{bmatrix} \\ &+ \begin{bmatrix} D_1(h_1^{n_1 n_2} * l * x_1)(n_0, n_1, n_2) \\ D_2(h_2^{n_1 n_2} * l * x_2)(n_0, n_1, n_2) \end{bmatrix}, \end{aligned} \quad (5)$$

where

$h_i^{m_1 m_2}(n_1, n_2)$: orientation mask at the pixel $(m_1, m_2)$ for the $i$-th morphogen,
$R_1(x_1, x_2)$, $R_2(x_1, x_2)$: the Brusselator reaction kinetics.

In the above equation, we define the orientation mask $h_1^{m_1 m_2}(n_1, n_2)$ at the pixel $(m_1, m_2)$ as a $32 \times 32$ matrix of real coefficients within the window $(n_1, n_2) = (-16, -16) \sim (15, 15)$. The mask $h_1^{m_1 m_2}(n_1, n_2)$ controls the dominant orientation of the generated pattern at every pixel $(m_1, m_2)$ according to the local ridge flow in the given fingerprint image. The orientation mask can be automatically derived as follows (Fig. 3): (i) take the

```
procedure Adaptive DRDS with Hierarchical Orientation Estimation
begin
  p := 2; { initialize the image partitioing factor}
  while time step n0 equals to 500 do
  begin
    if p is less than 9 then
    begin
      partition the input image into
      p^2 sub-images;
      generate independent orientation masks for
      p^2 sub-images;
      run the adaptive DRDS (Eq. (5)) for
      10 time steps;
      p := p + 1
    end
    else
    begin
      generate independent orientation masks
      for all pixels;
      run the adaptive DRDS (Eq. (5)) for
      10 time steps
    end
  end
end.
```

Figure 4: Algorithm for the adaptive DRDS with hierarchical orientation estimation.

Fourier transform of the local image around the pixel $(m_1, m_2)$, (ii) extract the dominant ridge orientation $\theta$ from the transformed image, (iii) generate a mask pattern $H_1^{m_1m_2}(j\omega_1, j\omega_2)$ having the orientation $\theta$ in frequency domain as

$$H_1^{m_1m_2}(j\omega_1, j\omega_2) = \begin{cases} 1 & \text{for unstable frequency band} \\ & \text{(black pixels in Fig. 3(iii))} \\ 2 & \text{otherwise,} \end{cases}$$

and (iv) take the inverse Fourier transform to obtain the orientation mask $h_1^{m_1m_2}(n_1, n_2)$. The orientation mask $h_2^{m_1m_2}(n_1, n_2)$ for the second morphogen, on the other hand, has the value 1 at the center $(n_1, n_2) = (0, 0)$, and equals to 0 for the other coordinates $(n_1, n_2)$. Thus, the dynamics for the morphogen $x_2(n_0, n_1, n_2)$ does not take account of the local orientation.

In practical situation, it is difficult to obtain the exact orientation masks from blurred fingerprints directly. Addressing this problem, we estimates local orientation masks recursively using a coarse-to-fine approach as shown in Fig. 4. This restoration algorithm starts with rough estimation of local orientation for four sub-images ($p = 2$). The image partitioning factor $p$ gradually increases as restoration step $n_0$ increases. We can obtain pixel-wise orientation masks $\boldsymbol{h}^{m_1m_2}(n_1, n_2)$ after 80 time steps. This simple strategy makes possible significant improvement in the precision of orientation estimation.

The problem considered here is to restore the original fingerprint image from its "subsampled" image. For this purpose, we generate a subsampled fingerprint image from the original image as follows: (i) partition the original image into $R\times S$-pixel rectangular blocks, and (ii) select one pixel randomly from every block and eliminate all the other pixels (set 127, middle gray-level, to the pixels). The image thus obtained has the same size as the original image, but the number of effective pixels is reduced to $1/(R\times S)$. Figure 5 shows the original image, the subsampled image ($n_0 = 0$) and restored images at $n_0 = 100$, 200 and 400, respectively, for the case of $1/(6 \times 6)$ subsampling. We can observe that the fingerprint pattern is reconstructed from the subsampled image gradually as time step $n_0$ increases.

## 4. SHORTEST PATH SEARCH

This section presents the shortest path search using the DRDS with FitzHugh-Nagumo (FHN) reaction kinetics, which is one of the most widely studied excitable model [7]. We shall define the FHN-based reaction kinetics for DRDS as

$$\begin{aligned} R_1(x_1, x_2) &= \frac{T_0}{k_1}\{x_1(x_1-k_2)(1-x_1)-x_2\}, \\ R_2(x_1, x_2) &= T_0\,(x_1 - k_3x_2)\,. \end{aligned} \tag{6}$$

In this paper, we employ the parameter set: $k_1 = 10^{-3}$, $k_2 = 10^{-6}$, $k_3 = 0.1$, $D_1 = 40$, $D_2 = 0$, $T_0 = 10^{-3}$ and $T_1 = T_2 = 1$.

The excitable DRDS exhibits spatio-temporal wave patterns. The excitable DRDS indicates the most important features of FHN dynamics; waves exhibit constant velocities and annihilate in collisions with boundaries or other waves. These features suggest a unique algorithm for the shortest path planning problems as described in [8]. Figure 6 shows a superposition of a excitable wave propagating through two-dimensional complex maze. A single propagating wave generates a map for finding the shortest path from a start point to any specified point in these maze.

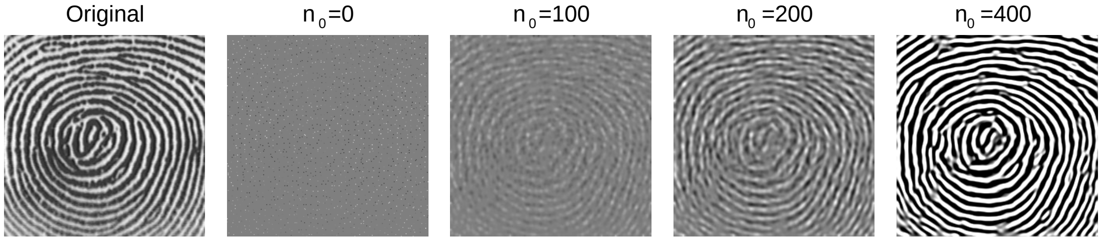


Figure 5: Fingerprint restoration from a subsampled image with subsampling rate $1/(6 \times 6)$.

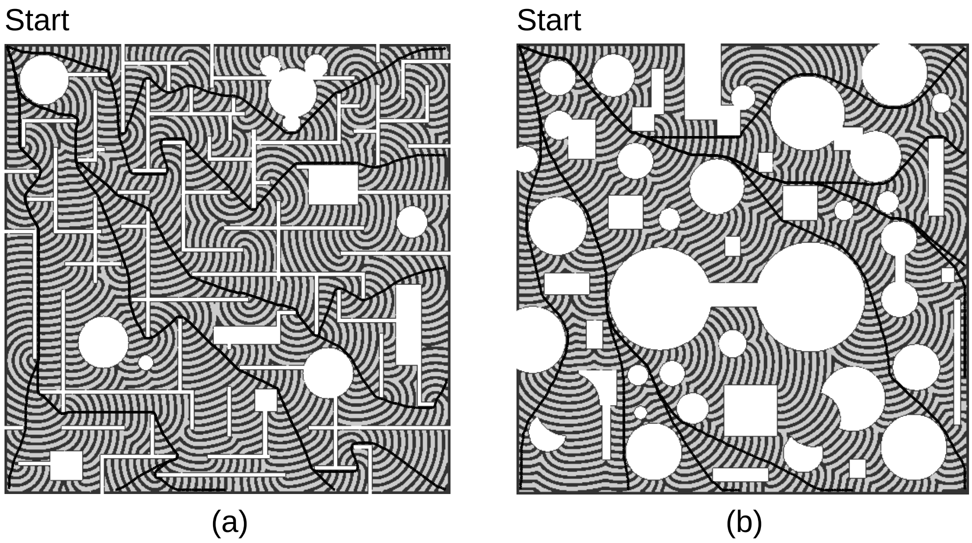


Figure 6: Results of shortest path search using DRDS.

## 5. CONCLUSION

This paper presents a digital reaction-diffusion system (DRDS) – a model of a discrete-time discrete-space reaction-diffusion dynamical system – useful for signal processing and computer graphics applications. We are expecting that the framework of DRDS may provide a theoretical foundation of *digital morphogenesis*, that is, a technique for applying the principle of biological pattern formation phenomena to many engineering problems.

## REFERENCES

[1] A. M. Turing,"The chemical basis of morphogenesis," *Phil. Trans. R. Soc. London*, Vol. B237, pp. 37–72, August 1952.

[2] K. R. Crounse and L. O. Chua,"Methods for image processing and pattern formation in cellular neural networks: a tutorial," *IEEE Trans. Circuits Syst.-I*, Vol. 42, No. 10, pp. 583–601, October 1995.

[3] L. Goras, L. O. Chua, and L. Pivka,"Turing patterns in cnns–part II: equations and behaviors," *IEEE Trans. Circuits Syst.-I*, Vol. 42, No. 10, pp. 612–626, October 1995.

[4] A. S. Sherstinsky and R. W. Picard,"M-lattice: From morphogenesis to image processing," *IEEE Trans. Image Processing*, Vol. 5, No. 7, pp. 1137–1150, July 1996.

[5] K. Ito, T. Aoki, and T. Higuchi,"Digital reaction-diffusion system —A foundation of bio-inspired texture image processing—," *IEICE Trans. Fundamentals*, Vol. E84-A, No. 8, pp. 1909–1918, August 2001.

[6] K. Ito, T. Aoki, and T. Higuchi,"Fingerprint restoration using digital reaction-diffusion system and its evaluation," *IEICE Trans. Fundamentals*, Vol. E86-A, No. 8, pp. 1916–1924, August 2003.

[7] J. D. Murray, *Mathematical Biology*,Springer-Verlag, 1993.

[8] O. Steinbock, Á. Tóth, and K. Showalter, "Navigating complex labyrinths: optimal paths from chemical waves," *Science*, Vol. 267, pp. 868–871, February 1995.